

Stable and Accurate Interpolation Operators for High-Order Multi-Block Finite-Difference Methods

K. Mattsson

Mark H. Carpenter

Abstract

Block-to-block interface interpolation operators are constructed for several common high-order finite difference discretizations. In contrast to conventional interpolation operators, these new interpolation operators maintain the strict stability, accuracy and conservation of the base scheme even when nonconforming grids or dissimilar operators are used in adjoining blocks. The stability properties of the new operators are verified using eigenvalue analysis, and the accuracy properties are verified using numerical simulations of the Euler equations in two spatial dimensions.

Key words: high-order finite difference methods, block interface, numerical stability, interpolation, adaptive grids

1 Introduction

Wave-propagation problems frequently require farfield boundaries to be positioned many wavelengths away from the disturbance source. To efficiently simulate these problems requires numerical techniques capable of accurately propagating disturbances over long distances. It is well known that high-order finite difference methods (HOFDM) are ideally suited for problems of this type. (See the pioneering paper by Kreiss and Oliger [13]). Not all high-order spatial operators are applicable, however. For example, schemes that are G-K-S stable [8], while being convergent to the true solution as $\Delta x \rightarrow 0$, may experience non-physical solution growth in time [3], thereby limiting their efficiency for long-time simulations. Thus, it is imperative to use HOFDMs that do not allow growth in time; a property termed “strict stability” [7]. Deriving strictly stable, accurate and conservative HOFDM is a significant

challenge and that has received considerable past attention. (For examples, see references [15, 32, 37, 29, 1, 2, 10, 30, 9]).

A robust and well-proven HOFD methodology that ensures the strict stability of time-dependent partial differential equations (PDEs) is the summation-by-parts simultaneous approximation term (SBP-SAT) method. The SBP-SAT method simply combines finite difference operators that satisfy a summation-by-parts (SBP) formula[12], with physical boundary conditions implemented using either the Simultaneous Approximation Term (SAT) method [3], or the projection method [27, 28, 19]. Examples of the SBP-SAT approach can be found in references [24, 23, 25, 18, 20, 22, 26, 17, 33, 34, 14, 5].

An added benefit of the SBP-SAT method is that it naturally extends to multi-block geometries while retaining the essential single-block properties: strict stability, accuracy and conservation [4]. Thus, problems involving complex domains or non-smooth geometries are easily amenable to the approach. References [17, 20, 35] report applications of the SBP-SAT HOFD methods to problems involving non-trivial geometries.

Current multi-block SBP-SAT methods suffer from two significant impediments: 1) the collocation points in adjoining blocks must match along block interfaces (i.e., “conforming” grids must be used), and 2) identical SBP schemes must be used tangential to the block interfaces.¹ These impediments prevent SBP-SAT operators from use on adaptively refined nonconforming multi-block grids and from use where hybrid-approaches involving two or more discretization techniques is desirable.

Although neither impediment (i.e., conforming grids or identical elements) significantly limits Finite- and Spectral-Elements methods,² to date, mitigating their influence in the context of HOFDM has rarely been successful. A noteworthy exception appears in reference [25], where a hybrid method is developed (based on the SBP-SAT technique) to merge a HOFDM to an unstructured finite-volume method. This was accomplished by alternating the finite volume scheme at the interface boundary.

The goals of the present study are two-fold. The first is to develop a systematic methodology for coupling arbitrary SBP methods between adjoining blocks. This task essentially requires identification of the conditions that adjoining interpolation operators must satisfy to guarantee interface strict stability, accuracy and conservation.

The second task is to demonstrate the new methodology by developing interface interpolation operators that couple commonly used SBP operators.

¹Ironically, these impediments were assumptions needed to prove stability and conservation, in the original single domain SBP-SAT approach.

²For example, see the nonconforming spectral multi-domain work of Kopriva and Kolas [11].

To this end, new interpolation operators are derived to couple 2nd-:2nd-, 4th-:4th-, 6th-:6th-, and 8th-:8th-order SBP operators across a nonconforming interface containing a 2 : 1 grid compression, as well as to couple 2nd-:4th- and 4th-:8th-order SBP operators across a conforming interface.

In Section 2 we introduce some definitions and discuss the SBP property. Sufficient conditions for the interface stability of a two-dimensional hyperbolic system are introduced in Section 3. The new approach utilizes the SAT technique in combination with newly developed SBP-preserving interpolation operators. The construction procedure for the SBP-preserving interpolation operators are presented in detail. In Section 4 the accuracy and stability properties of the newly developed multi-block interface coupling are tested by performing an eigenvalue analysis and numerical simulations of an analytic Euler vortex. In Section 5 conclusions are drawn. Sufficient conditions for interface stability of a 2D parabolic system followed by SBP-preserving interpolation operators are presented in the Appendix.

2 Definitions

Two- and three-dimensional schemes are constructed using tensor products of one-dimensional SBP finite-difference operators. Thus, we begin with a short description of 1D SBP operators including some relevant definitions. (For more details see [12, 31] and [18]).

2.1 Summation-By-Parts

Assume the existence of real-valued functions u, v such that $u, v \in \mathbf{L}^2[0, 1]$. Define an inner product to be $(u, v) = \int_0^1 u v dx$, and let the corresponding norm be $\|u\|^2 = (u, u)$. With these definitions, consider the hyperbolic scalar equation $u_t + u_x = 0$ (excluding the boundary condition). Apply the energy method to $u_t + u_x = 0$; i.e., multiplication by u and integration by parts leads to

$$\frac{d}{dt}\|u\|^2 = -(u, u_x) - (u_x, u) = -u^2|_0^1, \quad (1)$$

where $u^2|_0^1 \equiv u^2(x=1) - u^2(x=0)$.

Next, discretize the domain $(0 \leq x \leq 1)$ using $N+1$ equidistant grid points,

$$x_i = i h, \quad i = 0, 1, \dots, N, \quad h = \frac{1}{N}.$$

Denote the projection of v onto the discrete grid point x_i as v_i , and define the discrete solution vector to be $v^T = [v_0, v_1, \dots, v_N]$. As with the continuous inner product, define the discrete inner product for real-valued vector

functions $u, v \in \mathbf{R}^{N+1}$ to be $(u, v)_H = u^T H v$, where $H = H^T > 0$. The corresponding discrete norm becomes $\|v\|_H^2 = v^T H v$.

Definition 2.1 *A difference operator $D_1 = H^{-1}Q$ approximating $\partial/\partial x$ is a first-derivative SBP operator if $H = H^T$, $x^T H x > 0$, $x \neq 0$, and $Q + Q^T = B = \text{diag}(-1, 0 \dots, 0, 1)$.*

A semidiscretization of $u_t + u_x = 0$ is $v_t + D_1 v = 0$.

A semi-discrete energy for the system can be derived in a manner analogous to that used in the continuous case. That is, multiplying $v_t + D_1 v = 0$ from the left by $v^T H$ and adding the transpose leads to,

$$\frac{d}{dt} \|v\|_H^2 = -(v, H^{-1}Qv)_H - (H^{-1}Qv, v)_H = -v^T(Q + Q^T)v = v_0^2 - v_N^2. \quad (2)$$

Equation (2) is the discrete analog of (1).

Three definitions are central to the present study.

Definition 2.2 *An explicit p th-order accurate finite difference scheme with minimal stencil width of a Cauchy problem, is called a p th-order accurate narrow stencil.*

Definition 2.3 *A p th-order accurate narrow stencil SBP-operator is called a narrow-diagonal SBP operator if H is diagonal.*

Definition 2.4 *Let the row-vectors $\mathbf{x}^{\mathbf{k}}_f$ and $\mathbf{x}^{\mathbf{k}}_c$ be the projections of the polynomials x^k onto equidistant 1-D grids corresponding to a fine and coarse grid respectively. We say that I_{F2C} and I_{C2F} are p th-order accurate interpolation operators if $e_c^k \equiv I_{F2C}\mathbf{x}^{\mathbf{k}}_f - \mathbf{x}^{\mathbf{k}}_c$ and $e_f^k \equiv I_{C2F}\mathbf{x}^{\mathbf{k}}_c - \mathbf{x}^{\mathbf{k}}_f$ vanish for $k = 0..p-1$ in the interior and for $k = 0 \dots (p-1)/2$ at the boundaries.*

Remark The boundary closure for a p th-order accurate narrow-diagonal SBP operator is of order $p/2$ (see [18]). The convergence rate for narrow stencil approximations of fully hyperbolic problems (e.g., the Eulers equations) drops to $(p/2 + 1)$ th-order. (See refs. [6, 36] for more information on the accuracy of finite difference approximations).

Remark We state here without proof that the accuracy of the p th-order narrow-diagonal SBP operator is preserved when using the p th-order accurate interpolation operators. Numerical experiments presented later herein, are consistent with this conjecture.

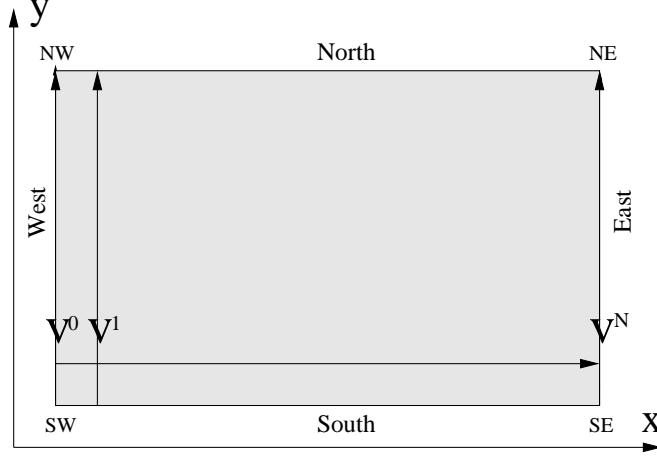


Figure 1: Domain 2-D

2.2 Two-Dimensional Domains

We begin by introducing the Kronecker product

$$C \otimes D = \begin{bmatrix} c_{0,0} D & \cdots & c_{0,q-1} D \\ \vdots & & \vdots \\ c_{p-1,0} D & \cdots & c_{p-1,q-1} D \end{bmatrix},$$

where C is a $p \times q$ matrix and D is an $m \times n$ matrix. Two useful rules for the Kronecker product are $(A \otimes B)(C \otimes D) = (AC) \otimes (BD)$ and $(A \otimes B)^T = A^T \otimes B^T$.

Next, consider the 2-D rectangular domain $\Omega_{d,u}^{l,r}$ bounded by $l \leq x \leq r$, $d \leq y \leq u$ with an $(N+1) \times (M+1)$ -point equidistant grid defined as,

$$\begin{aligned} x_i &= ih_x, \quad i = 0, 1, \dots, N, \quad h_x = \frac{r-l}{N}, \\ y_j &= jh_y, \quad j = 0, 1, \dots, M, \quad h_y = \frac{u-d}{M}. \end{aligned}$$

The numerical approximation at grid point (x_i, y_j) is a $1 \times k$ -vector denoted $v_{i,j}$. The tensor product derivations are more transparent if we redefine the component vector $v_{i,j}$ as a “vector of vectors”. Specifically, define a discrete solution vector $v^T = [v^0, v^1, \dots, v^N]$, where $v^p = [v_{p,0}, v_{p,1}, \dots, v_{p,M}]$ is the solution vector at x_p along the y-direction, illustrated in Figure 1. To distinguish whether a difference operator P is operating in the x - or the y -direction we use the notations P^x and P^y . The following two-dimensional

operators are frequently used,

$$\begin{aligned} \mathbf{D}^x &= (D^x \otimes I^y), & \mathbf{D}^y &= (I^x \otimes D^y) \\ \mathbf{H}^x &= (H^x \otimes I^y), & \mathbf{H}^y &= (I^x \otimes H^y) \\ \mathbf{e}_0^x &= (e_0 \otimes I^y), & \mathbf{e}_0^y &= (I^x \otimes e_0) \\ \mathbf{e}_N^x &= (e_N \otimes I^y), & \mathbf{e}_M^y &= (I^x \otimes e_M) \end{aligned} \quad , \quad (3)$$

where $D^{x,y}$, and $H^{x,y}$ are the one-dimensional operators in the x- and y-direction, respectively, $I^{x,y}$ are identity matrices of appropriate sizes, and e_0 , and e_N are one-dimensional “boundary” vectors defined by

$$e_0 = [1, 0, \dots, 0]^T, \quad e_N = [0, \dots, 0, 1]^T. \quad (4)$$

3 Analysis

Our main focus is on multi-block interface coupling solving PDEs on non-conforming grids, combining different (here referring to the formal order of accuracy) finite difference SBP schemes.

Consider the following 2-D hyperbolic problem (the extension to parabolic problems is shown in the Appendix):

$$\begin{aligned} \mathbf{u}_t + A\mathbf{u}_x + B\mathbf{u}_y &= 0, & \mathbf{x} &\in \Omega_{d,u}^{l,i}, \\ \mathbf{v}_t + A\mathbf{v}_x + B\mathbf{v}_y &= 0, & \mathbf{x} &\in \Omega_{d,u}^{i,r} \end{aligned} \quad , \quad (5)$$

where A and B are symmetric $k \times k$ matrices ($k = 4$ for the compressible Euler equations). (The extension of the present study to 3-D is straightforward.) A corresponding semi-discrete approximation of (5) can be written

$$\begin{aligned} u_t + A \otimes \mathbf{D}_L^x u + B \otimes \mathbf{D}_L^y u &= SAT_{IL}^I + SAT_L^I \\ v_t + A \otimes \mathbf{D}_R^x v + B \otimes \mathbf{D}_R^y v &= SAT_{IR}^I + SAT_R^I, \end{aligned} \quad (6)$$

where $SAT_{L,R}^I$ denote the penalty terms at the outer boundaries. (These are tuned to obtain stability, see [24, 22, 35] for details.) The penalty terms handling the multi-block coupling can be written as

$$\begin{aligned} SAT_{IL}^I &= \Sigma_L \otimes (\mathbf{H}_L^x)^{-1} \mathbf{e}_N^x \{u_N - I_k \otimes I_{F2C} v_0\} \\ SAT_{IR}^I &= \Sigma_R \otimes (\mathbf{H}_R^x)^{-1} \mathbf{e}_0^x \{v_0 - I_k \otimes I_{C2F} u_N\} \end{aligned} \quad . \quad (7)$$

(However, the penalty terms (7) is not the most general representation, as will be shown later in this section.) The continuity condition $u - v = 0$ along

the interface (at x_i) is approximated by $u_N - I_k \otimes I_{F2C} v_0$ and $v_0 - I_k \otimes I_{C2F} u_N$ in the above penalty-terms. Σ_R and Σ_L are unknown $k \times k$ matrices to be determined below by stability. We use the subscripts L, R to distinguish the operators in the left and right domain (which can be completely unrelated, i.e., we can use different numerical schemes in the two domains), with the only assumption that they fulfill the SBP property. I_{F2C} and I_{C2F} are 1-D interpolation operators constructed such that $I_k \otimes I_{F2C} v_0$ and $I_k \otimes I_{C2F} u_N$ have the same dimension as u_N and v_0 respectively. u_N and v_0 are $km \times 1$ vectors with components aligned with the block interface. For future reference we introduce the following norms:

$$M_L = (I_k \otimes H_L^x \otimes H_L^y), \quad M_R = (I_k \otimes H_R^x \otimes H_R^y), \quad (8)$$

and the following terms:

$$IT^I = \begin{array}{cc} -u_N^T (A \otimes H_L^y) u_N & + v_0^T (A \otimes H_R^y) v_0 \\ + 2u_N^T (\Sigma_L \otimes H_L^y) u_N & + 2v_0^T (\Sigma_R \otimes H_R^y) v_0 \\ - u_N^T (\Sigma_L \otimes H_L^y I_{F2C}) v_0 & - v_0^T (\Sigma_R \otimes H_R^y I_{C2F}) u_N \\ - u_N^T (\Sigma_R \otimes I_{C2F}^T H_R^y) v_0 & - v_0^T (\Sigma_L \otimes I_{F2C}^T H_L^y) u_N \end{array}, \quad (9)$$

$$X = \begin{bmatrix} H_L^y & -H_L^y I_{F2C} \\ -H_R^y I_{C2F} & H_R^y \end{bmatrix}, \quad w^T = \begin{bmatrix} u_N \\ v_0 \end{bmatrix}. \quad (10)$$

We introduce the following important relations,

$$H_R^y I_{C2F} = I_{F2C}^T H_L^y, \quad (11)$$

$$H_L^y (I_L^y - I_{F2C} I_{C2F}) \geq 0, \quad H_R^y (I_R^y - I_{C2F} I_{F2C}) \geq 0, \quad (12)$$

where $I_{L,R}^y$ are identity matrices of appropriate sizes. The following definition is central to the present study,

Definition 3.1 *A p th-order accurate interpolation operator that fulfills (11) is called a p th-order accurate SBP-preserving interpolation operator.*

The following lemma is central to the present study:

Lemma 3.2 *The scheme (6) with the penalty terms given by (7) is stable if $2\Sigma_L = A$, $2\Sigma_R = -A$ and (11) hold, assuming that the boundary terms $SAT_{L,R}^I$ are correctly implemented.*

Proof Apply the energy method by multiplying the first and second equation in (6) by $u^T M_L$ and $v^T M_R$ (defined by (8)) respectively, yielding,

$$\frac{d}{dt}(\|u\|_{M_L} + \|v\|_{M_R}) = BT^I + IT^I,$$

where BT^I corresponds to the outer boundary terms (which we assume are correctly implemented, i.e., bounded) and IT^I corresponds to the multi-block interface coupling given by (9).

A stable coupling is obtained if IT^I is non-positive. A non-dissipative and stable coupling is achieved by choosing

$$2\Sigma_L = A, \quad 2\Sigma_R = -A, \quad H_R^y I_{C2F} = I_{F2C}^T H_L^y,$$

which makes $IT^I = 0$. \square

Remark Note the critical relationship that equation (11) imposes on the two interface interpolation operators. Indeed, the two conditions $2\Sigma_L = A$, $2\Sigma_R = -A$ and equation (11) provide sufficient conditions for interface stability.

Remark Another important interface property is conservation, especially for problems with discontinuous solutions. Indeed, the Lax-Wendroff theorem relates discrete conservation to convergence to the weak solution of the differential equation. It is shown in [4, 23] for conforming grids that conservation provides a necessary condition for interface stability. Likewise, the conditions for conservation are fulfilled by imposing the necessary conditions for stability in Lemma 3.2 (or Lemma 3.3).

For non-linear problems (such as the compressible Euler equations) characteristic boundary conditions are often imposed (since they introduce damping [20] at the boundaries) which can also be utilized at block interfaces (see for example [20, 35]). Since A is a symmetric matrix, it can be diagonalized by $R^T A R = \Lambda$, where R is a matrix consisting of the eigenvectors of A . We introduce the notation $\bar{A} \equiv R|\Lambda|R^T$, and $2A^\pm \equiv A \pm \bar{A}$. (The matrix B is also symmetric and can be rotated to diagonal form with a similar transformation.) To couple characteristic variables using the SAT technique [20, 35] at the block-interface we choose $\Sigma_L = A^-$, $\Sigma_R = -A^+$.

The following lemma states the stability conditions for a characteristic multi-block coupling:

Lemma 3.3 *The scheme (6) with the penalty terms given by (7) is stable if $\Sigma_L = A^-$, $\Sigma_R = -A^+$, (11) and (12) hold, assuming that the boundary terms $SAT_{L,R}^I$ are correctly implemented.*

Proof Apply the energy method by multiplying the first and second equation in (6) by $u^T M_L$ and $v^T M_R$ (defined by (8)) respectively, yielding,

$$\frac{d}{dt}(\|u\|_{M_L} + \|v\|_{M_R}) = BT^I + IT^I,$$

where BT^I corresponds to the outer boundary terms (which we assume are correctly implemented, i.e., bounded) and IT^I corresponds to the multi-block interface coupling given by (9).

A stable coupling is obtained if IT^I is non-positive. If $\Sigma_L = A^-$, $\Sigma_R = -A^+$ and $H_R^y I_{C2F} = I_{F2C}^T H_L^y$ hold, $IT^I = -\bar{A} \otimes w^T X w$ where w^T and X are given by (10). (By assumption $H_L^y I_{F2C} = (H_R^y I_{C2F})^T$ which makes X symmetric.) Hence, stability follows if X is positive semi-definite, since \bar{A} is a symmetric and positive semi-definite matrix. Sylvester's theorem states that $X \geq 0$ if the following conditions hold:

$$\begin{aligned} H_L^y &> 0, \quad H_L^y - H_L^y I_{F2C} (H_R^y)^{-1} H_R^y I_{C2F} \geq 0 \\ H_R^y &> 0, \quad H_R^y - H_R^y I_{C2F} (H_L^y)^{-1} H_L^y I_{F2C} \geq 0 \end{aligned}.$$

By definition $H_L^y > 0$, $H_R^y > 0$. Hence stability follows if (12) holds. \square

The extra conditions in (12), besides the necessary conditions in (11) introduce a significant restriction in the construction of the interpolation operators (as will be shown in the coming section). The energy estimate for the characteristic coupling (as described in Lemma 3.3) gave us an idea how to remove the extra conditions (12) and yet introduce a damping mechanism by the penalty coupling. Consider the following energy estimate

$$\frac{d}{dt}(\|u\|_{M_L} + \|v\|_{M_R}) = BT^I - \Omega \otimes w^T X^\alpha w, \quad (13)$$

where Ω is symmetric and positive definite and α is a positive integer (w^T and X are given by (10)). For $\Omega = \bar{A}$ and $\alpha = 1$ we recover the energy estimate from the characteristic coupling, presented in Lemma 3.3. By choosing α an even integer, stability follows if X is symmetric (which is true if condition (11) holds), regardless of the extra conditions in (12). We introduce the

following penalties:

$$\begin{aligned}
SAT_{IL}^I &= + \frac{A}{2} \otimes (\mathbf{H}_L^x)^{-1} \mathbf{e}_N^x \{u_N - I_k \otimes I_{F2C} v_0\} \\
&\quad - \Omega \otimes (\mathbf{H}_L^x)^{-1} \mathbf{H}_L^y \mathbf{e}_N^x \{u_N - I_k \otimes I_{F2C} v_0\} \\
&\quad - \Omega \otimes (\mathbf{H}_L^x)^{-1} \mathbf{I}_{F2C} \mathbf{H}_R^y \mathbf{e}_N^x \{I_{C2F} u_N - v_0\} \\
SAT_{IR}^I &= - \frac{A}{2} \otimes (\mathbf{H}_R^x)^{-1} \mathbf{e}_0^x \{v_0 - I_k \otimes I_{C2F} u_N\} \\
&\quad - \Omega \otimes (\mathbf{H}_R^x)^{-1} \mathbf{H}_R^y \mathbf{e}_0^x \{v_0 - I_k \otimes I_{C2F} u_N\} \\
&\quad - \Omega \otimes (\mathbf{H}_R^x)^{-1} \mathbf{I}_{C2F} \mathbf{H}_L^y \mathbf{e}_0^x \{I_{F2C} v_0 - u_N\}
\end{aligned} \tag{14}$$

The first two penalty terms in (14) (i.e., the first in SAT_{IL}^I and the first in SAT_{IR}^I) are identical to the non-dissipative penalty coupling defined in Lemma 3.2. The following lemma resolves the issue with the extra conditions in (12),

Lemma 3.4 *The scheme (6) with the penalty terms given by (14) is stable if Ω is symmetric and positive definite and (11) holds, assuming that the boundary terms $SAT_{L,R}^I$ are correctly implemented.*

Proof Apply the energy method by multiplying the first and second equation in (6) by $u^T M_L$ and $v^T M_R$ (defined by (8)) respectively, leading to (13), with $\alpha \equiv 2$. BT^I corresponds to the outer boundary terms (which we assume are correctly implemented, i.e., bounded). Stability follows if Ω is symmetric and positive definite. \square

Lemma 3.4 is validated numerically in Appendix I, where we also show that condition (11) is necessary to guarantee a stable characteristic coupling.

Remark For non-linear phenomena the addition of artificial dissipation (AD) is often required for stability. The addition of SBP preserving AD [21] does not alter the stability conditions in Lemma 3.2, Lemma 3.3 or Lemma 3.4.

3.1 Construction of Interpolation Operators

This section briefly describes the construction of the SBP-preserving interpolation operators I_{F2C} and I_{C2F} . In the present study we will consider a two to one ratio between the coarse and the fine grids along the common interface. (The analysis is not restricted to a two to one ratio, it merely

simplifies the construction.) The structure (here showing the upper part) of the interpolation operator I_{F2C} is given by:

$$\begin{pmatrix} a_{1,1} & & \cdots & & \cdots & & \cdots & & \cdots & & a_{1,r} \\ \vdots & & & & & & & & & & \vdots \\ a_{q,1} & & \cdots & & \cdots & & \cdots & & & & a_{q,r} \\ a_{2s} & a_{2s-1} & a_{2s-2} & \cdots & a_0 & \cdots & a_{2s-2} & a_{2s-1} & a_{2s} & & \\ & & a_{2s} & a_{2s-1} & a_{2s-2} & \cdots & a_0 & \cdots & a_{2s-2} & a_{2s-1} & a_{2s} \\ & & & \ddots & & \ddots & & \ddots & & \ddots & \ddots \end{pmatrix}$$

(The lower part of I_{F2C} is obtained by a permutation of both rows and columns.) The other interpolation operator is given by $I_{C2F} = (H_L^y)^{-1}(H_R^y I_{F2C})^T$. For example, in the fourth-order case (see the Appendix) we have used $q = 3, r = 11$ and $s = 2$, which leads to the following form:

$$I_{C2F} = \begin{pmatrix} b_{1,1} & \cdots & & & b_{1,8} \\ \vdots & & & & \vdots \\ b_{11,1} & \cdots & & & b_{11,8} \\ & & 2a_3 & 2a_1 & 2a_1 & 2a_3 \\ & & 2a_4 & 2a_2 & 2a_0 & 2a_2 & 2a_4 \\ & & & & 2a_3 & 2a_1 & 2a_1 & 2a_3 \\ & & & & 2a_4 & 2a_2 & 2a_0 & 2a_2 & 2a_4 \\ & & & & \ddots & & \ddots & & \ddots \end{pmatrix}$$

(The lower part of I_{C2F} is obtained by a permutation of both rows and columns.) Notice that the unknowns in I_{C2F} are completely defined by the unknowns in I_{F2C} and the known coefficients in H_L^y and H_R^y .

Remark A pth -order accurate interpolation operator will preserve the order of the finite difference scheme (6) utilizing narrow-diagonal SBP operators, i.e., resulting in $(p/2+1)th$ order accuracy. SBP discretizations not restricted (see for example [18, 31]) to a $(p/2)th$ -order accurate boundary stencil, require a more accurate boundary closure of the interpolation operators to maintain the convergence rate. We omit a detailed study (see [36] for more information on the accuracy of finite difference approximations) of the accuracy requirement.

The following procedure describes the construction of the pth -order accurate interpolation operators, given the y -norms in the left (H_L^y) and right (H_R^y) domains:

- Build I_{F2C} with the form given above.
- Build $I_{C2F} = (H_R^y)^{-1} I_{F2C}^T H_L^y$, given H_L^y and H_R^y .
- Solve for accuracy (see Definition 2.4).

(In step 2 above we have assumed that the left domain corresponds to the coarse grid, if not simply replace the positions between H_L^y and H_R^y if we have the opposite scenario.) If there are free parameters left after imposing the accuracy conditions they are tuned to obtain an optimal L_2 error. For the p th-order accurate case this means that $e_k^2 \equiv (e_c^k)^T \cdot e_c^k + (e_f^k)^T \cdot e_f^k$ (see Definition 2.4) is optimized for $k = (p - 1)/2 + 1 \dots$ (resulting in linear equations to be solved) until there are no free parameters left.

With these assumptions there exist by construction SBP-preserving interpolation operators for the second, fourth, sixth and eighth order cases (based on narrow-diagonal SBP schemes), by using the symbolic mathematics software Maple, (see the Appendix). We have also constructed interpolation operators coupling fourth to second and eighth to fourth-order accurate SBP discretizations.

Remark This is the first time (to our knowledge) that stability for multi-block coupling of finite difference schemes with different order of accuracy in more than 1-D have been shown.

For the second-order and fourth-order cases the constructed interpolation operators fulfill the extra conditions in (12), besides the necessary conditions in (11). It is an open question if the conditions in (12) can be met for the sixth and eighth-order cases.

4 Computations

We perform some numerical tests to verify the accuracy and stability properties of the SBP-preserving interpolation operators.

4.1 Numerical Validation of Lemma 3.2

To test the stability properties numerically we can either perform : 1) a long-time integration, or 2) an eigenvalue analysis. We chose the latter in the present study. Consider (6) with the following setup:

$$\begin{aligned}
 A = B = \begin{bmatrix} 1 & 0 \\ 0 & -1 \end{bmatrix}, \quad u = \begin{bmatrix} u^{(0)} \\ u^{(1)} \end{bmatrix} \quad v = \begin{bmatrix} v^{(0)} \\ v^{(1)} \end{bmatrix} \\
 u^{(0)} = u^{(1)}, \quad v^{(0)} = v^{(1)} : \quad \text{at the outer boundaries} \quad \cdot \quad (15) \\
 u^{(0)} = v^{(0)}, \quad u^{(1)} = v^{(1)} : \quad \text{at the block-interface}
 \end{aligned}$$

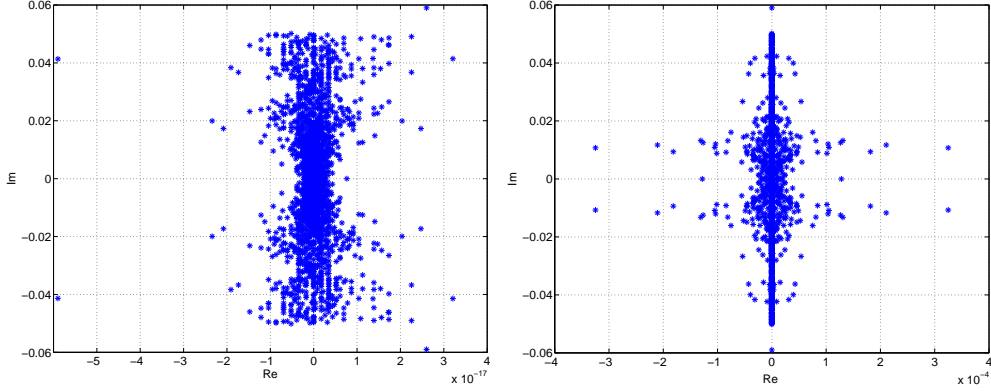


Figure 2: The spectrum of the discrete approximation to (15) multiplied by h_R for the fourth-order discretization, with stable SBP-preserving interpolation (left) and unstable non-SBP interpolation (right). 15^2 unknowns in the left (coarse) block. (Notice the different scales.)

Despite its simplicity, this model problem is very challenging to solve numerically (without introduction of artificial damping) since it is energy-conserving, i.e., the eigenvalues are purely imaginary (see [16] for details). This makes it an ideal benchmark problem testing for stability of a certain numerical scheme, including boundaries.

The eigenvalues of the numerical approximation of the continuous test-problem (given by (5) and (15)) employing SBP-preserving interpolation operators fulfilling the conditions in (11) for the fourth (using 15^2 unknowns in the left (coarse mesh) region) and the sixth (using 21^2 unknowns in the left (coarse mesh) region) order accurate cases are shown in Figures 2 and 3 respectively. We have multiplied the eigenvalues with the grid-size (h_R) of the fine-mesh domain. (The interpolation operators are presented in the Appendix.) To further indicate the importance of Lemma 3.2 we also present the corresponding results employing interpolation operators that do not fulfill the conditions in (11) (and hence a violation to Lemma 3.2), referred to as non-SBP interpolation.

The non-SBP interpolation operators as compared to the corresponding SBP-preserving interpolation operator fulfilling the conditions in (11) differ only at the boundaries. The boundary closures of the non-SBP interpolation operators (presented in the Appendix) are defined by the following two requirement: 1) to have the same formal accuracy at all grid-points, and 2) to use a minimal stencil width. The non-SBP interpolation operators clearly introduce an instability due to eigenvalues to the right of the imaginary axis.

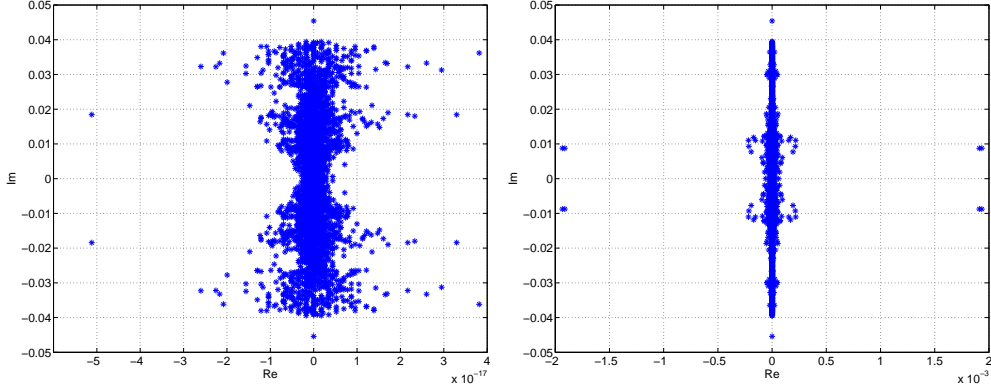


Figure 3: The spectrum of the discrete approximation to (15) multiplied by h_R for the sixth-order discretization, with stable SBP interpolation (left) and unstable non-SBP interpolation (right). 21^2 unknowns in the left (coarse) block. (Notice the different scales.)

4.2 Vortex in Free Space

To test the accuracy of the present method a 2-D Euler-vortex (an analytic solution [20] to the compressible Euler equations) is run across a multi-block interface. The problem consists of 2 blocks (5×5 unit area) having non-matching gridlines. The blocks are patched together according to (6). We set the Mach number $Ma = 0.3$. The vortex is initiated at $x=4$ (one unit to the left of the interface at $x=5$) with a 10 degree angle of the background free-stream and then propagated to $t = 1$, see Figure 4.

The convergence rate is calculated as

$$q = \log_{10} \left(\frac{\|w - w^{(h_1)}\|_h}{\|w - w^{(h_2)}\|_h} \right) / \log_{10} \left(\frac{h_1}{h_2} \right), \quad (16)$$

where w is the analytic solution and $w^{(h_1)}$ the corresponding numerical solution with grid size h_1 . $\|w - w^{(h_1)}\|_h$ is the discrete l_2 norm of the error. Since the solution consists of 2 blocks we add together the two different l_2 -errors. The standard explicit 4th-order Runge-Kutta method is used for time integration.

The convergence results going from coarse to fine grid using second, fourth, sixth and eighth-order accurate schemes are presented in Tables 1-4. (The number M is the number of unknowns in the y-direction in the coarse grid.)

The potential gain of a hybrid approach (here referring to the multi-block coupling of a higher order scheme on a coarse-grid domain to a lower order

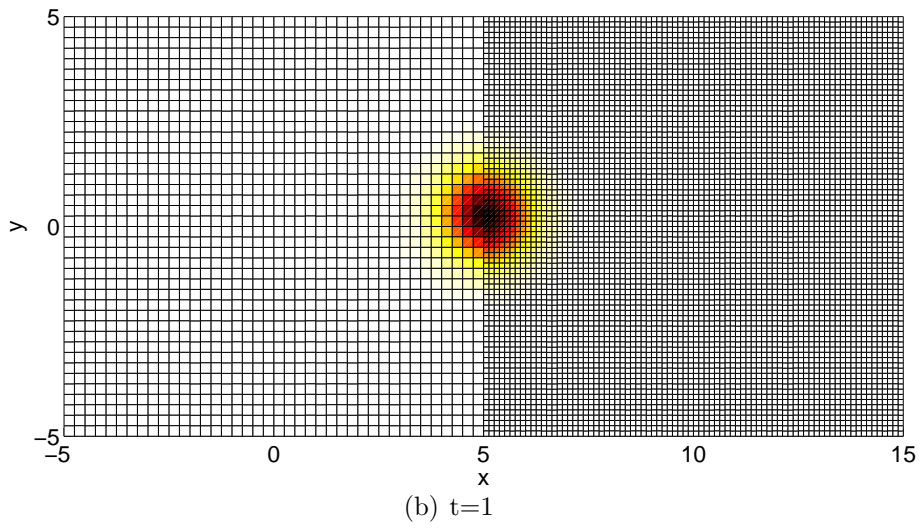
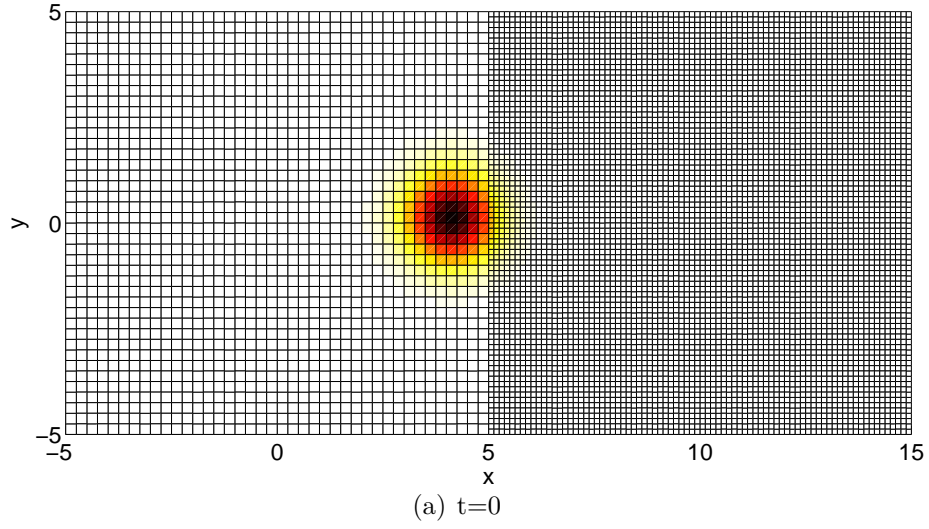


Figure 4: Pressure contours for the vortex at $t=0$ (initial data) and at $t = 1$, computed with the sixth-order method using 41×41 grid points in the coarse (left domain).

| M | $\log(\rho)$ | $q^{(\rho)}$ | $\log(l_2(u))$ | $q^{(u)}$ | $\log(l_2(v))$ | $q^{(v)}$ | $\log(l_2(p))$ | $q^{(p)}$ |
|-----|--------------|--------------|----------------|-----------|----------------|-----------|----------------|-----------|
| 51 | -4.16 | — | -3.43 | — | -3.16 | — | -3.22 | — |
| 101 | -4.76 | 2.00 | -4.04 | 2.02 | -3.78 | 2.04 | -3.82 | 2.01 |
| 151 | -5.12 | 2.00 | -4.39 | 2.01 | -4.13 | 2.02 | -4.18 | 2.00 |

Table 1: l_2 -error and convergence rate q . Second order case. Coarse to fine grid. $Ma = 0.3$. Vortex centered at interface at $t = 1$.

| M | $\log(\rho)$ | $q^{(\rho)}$ | $\log(l_2(u))$ | $q^{(u)}$ | $\log(l_2(v))$ | $q^{(v)}$ | $\log(l_2(p))$ | $q^{(p)}$ |
|-----|--------------|--------------|----------------|-----------|----------------|-----------|----------------|-----------|
| 51 | -4.61 | — | -4.22 | — | -3.85 | — | -3.80 | — |
| 101 | -5.53 | 3.07 | -5.12 | 2.99 | -4.79 | 3.13 | -4.70 | 2.99 |
| 151 | -6.07 | 3.05 | -5.65 | 2.99 | -5.33 | 3.08 | -5.23 | 3.01 |

Table 2: l_2 -error and convergence rate q . Fourth order case. Coarse to fine grid. $Ma = 0.3$. Vortex centered at interface at $t = 1$.

| M | $\log(\rho)$ | $q^{(\rho)}$ | $\log(l_2(u))$ | $q^{(u)}$ | $\log(l_2(v))$ | $q^{(v)}$ | $\log(l_2(p))$ | $q^{(p)}$ |
|-----|--------------|--------------|----------------|-----------|----------------|-----------|----------------|-----------|
| 51 | -5.13 | — | -4.38 | — | -4.04 | — | -4.25 | — |
| 101 | -6.27 | 3.79 | -5.66 | 4.25 | -5.30 | 4.19 | -5.53 | 4.24 |
| 151 | -7.02 | 4.24 | -6.44 | 4.44 | -6.09 | 4.48 | -6.29 | 4.33 |

Table 3: l_2 -error and convergence rate q . Sixth order case. Coarse to fine grid. $Ma = 0.3$. Vortex centered at interface at $t = 1$.

| M | $\log(\rho)$ | $q^{(\rho)}$ | $\log(l_2(u))$ | $q^{(u)}$ | $\log(l_2(v))$ | $q^{(v)}$ | $\log(l_2(p))$ | $q^{(p)}$ |
|-----|--------------|--------------|----------------|-----------|----------------|-----------|----------------|-----------|
| 51 | -4.72 | — | -4.44 | — | -3.93 | — | -4.00 | — |
| 101 | -6.07 | 4.48 | -5.84 | 4.66 | -5.39 | 4.83 | -5.30 | 4.30 |
| 151 | -6.93 | 4.87 | -6.67 | 4.75 | -6.27 | 5.04 | -6.13 | 4.74 |

Table 4: l_2 -error and convergence rate q . Eighth order case. Coarse to fine grid. $Ma = 0.3$. Vortex centered at interface at $t = 1$.

| M | $\log(\rho)$ | $q^{(\rho)}$ | $\log(l_2(u))$ | $q^{(u)}$ | $\log(l_2(v))$ | $q^{(v)}$ | $\log(l_2(p))$ | $q^{(p)}$ |
|-----|--------------|--------------|----------------|-----------|----------------|-----------|----------------|-----------|
| 51 | -4.53 | — | -4.12 | — | -3.75 | — | -3.72 | — |
| 101 | -5.28 | 2.51 | -4.81 | 2.30 | -4.47 | 2.39 | -4.45 | 2.45 |
| 151 | -5.68 | 2.23 | -5.18 | 2.11 | -4.85 | 2.13 | -4.84 | 2.21 |

Table 5: l_2 -error and convergence rate q . Fourth to second-order case. Coarse to fine grid. $Ma = 0.3$. Vortex centered at interface at $t = 1$.

| M | $\log(\rho)$ | $q^{(\rho)}$ | $\log(l_2(u))$ | $q^{(u)}$ | $\log(l_2(v))$ | $q^{(v)}$ | $\log(l_2(p))$ | $q^{(p)}$ |
|-----|--------------|--------------|----------------|-----------|----------------|-----------|----------------|-----------|
| 51 | -4.74 | — | -4.43 | — | -3.93 | — | -4.01 | — |
| 101 | -6.07 | 4.41 | -5.82 | 4.60 | -5.38 | 4.81 | -5.29 | 4.25 |
| 151 | -6.89 | 4.69 | -6.63 | 4.63 | -6.25 | 4.96 | -6.11 | 4.65 |

Table 6: l_2 -error and convergence rate q . Eighth to Fourth order case. Coarse to fine grid. $Ma = 0.3$. Vortex centered at interface at $t = 1$.

scheme on a fine-grid domain) is found by comparing the results (which are almost identical) in Tables 6 and 4. In Table 6 we couple an eighth-order accurate SBP scheme in the left (coarse) domain to a fourth-order accurate SBP scheme in the right (fine) domain. In Table 4 the eighth-order stencil is used in both domains. In Table 5 we couple a fourth-order accurate SBP scheme in the left (coarse) domain to a second-order accurate SBP scheme in the right (fine) domain. A comparison of Tables 5 and 2 indicates the benefit of employing higher (than second) order accurate methods for wave dominated problems (the error of the second order schemes clearly dominates).

5 Conclusions

Our approach have been to use SBP operators, the SAT technique and SBP-preserving interpolation operators to enforce the interface conditions in a stable and accurate way for general hyperbolic (and parabolic) problems, defined on nonconforming grids. The main objective was to construct interpolation operators that combined the following desirable properties:

- Stability by construction without interfering with the existing SBP schemes.
- Maintaining the overall convergence rate.
- Maintaining simplicity of the numerical scheme.

To achieve the three properties above, we have constructed interpolation operators with the following requirements: i) They preserve the summation by parts rule based on the underlying SBP scheme. ii) They have the same order of accuracy as the underlying SBP scheme. iii) They are of minimal width in the interior.

Numerical computations for the 2-D compressible Euler equations corroborate the stability and accuracy properties and also show that a careful boundary treatment is necessary to guarantee stability of the interface coupling.

6 Acknowledgments

We would like to thank Jan Nordström for very useful discussions, comments and suggestions throughout this work. Jan Nordström have made significant contributions in the framework of hybrid multi-block couplings of various SBP schemes utilizing the SAT technique. His earlier contributions have been a vital part in the development of the present study.

APPENDIX

I Numerical Validation of Lemma 3.3 and Lemma 3.4

In this section we verify numerically the necessity of the extra conditions (12) that turned up in Lemma 3.3. We will also verify the modified penalties (14) that removed the necessity of conditions (12), in order to obtain an energy estimate, yet introducing a dissipative coupling (referring to the energy estimate (13)).

Consider (6) with the setup given by (15). The scheme (6) with the penalty terms given by (7) was proven stable if $\Sigma_L = A^-$, $\Sigma_R = -A^+$, assuming that both the conditions in (11) and (12) hold. However, for the sixth-order case condition (12) could not be met. This led us to consider the scheme (6) with the penalty terms instead given by (14), where stability follows if Ω is symmetric and positive definite. In the present study we use $\Omega = \bar{A}$. The two different schemes (that differ only in how the SAT coupling is done) will be referred to as the characteristic coupling and the quadratic coupling.

The eigenvalues of the two different numerical approximations (the characteristic coupling and the quadratic coupling) employing the SBP-preserving interpolation operators fulfilling the conditions in (11) for the sixth- (using 21^2 unknowns in the left (coarse mesh) region) order accurate cases are shown in Figure 5 (compare with the corresponding non-dissipative coupling, presented in Figure 3). We have multiplied the eigenvalues with the grid-size (h_R) of the fine-mesh domain. A closer look at the eigenvalues for the characteristic coupling reveals some eigenvalues with a positive real part, the largest of order 10^{-4} . This is a strong indication that when employing a characteristic coupling the conditions in (12) is necessary. (The interpolation operators for the second and fourth order accurate cases do obey the extra conditions in (12). We have verified, although not presented here, that the second- and fourth-order accurate cases does not have eigenvalues with positive real part for the characteristic coupling). The quadratic coupling (not required to obey (12)) on the other hand results in eigenvalues having non-positive real parts, in agreement with Lemma 3.4.

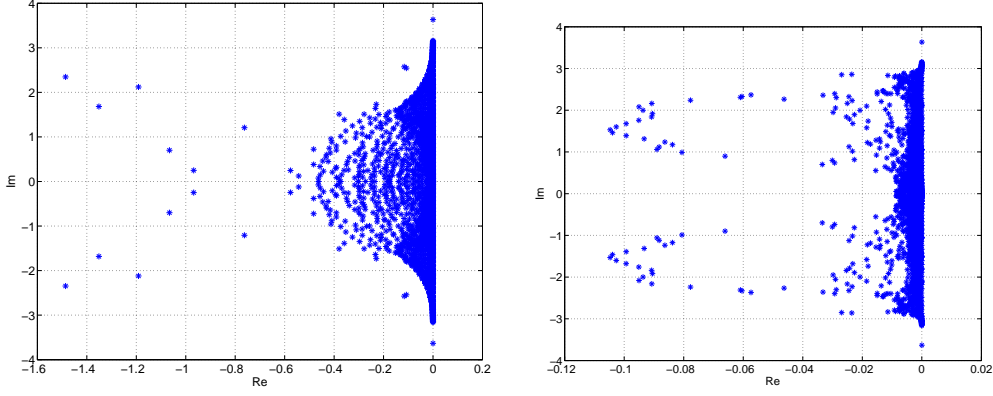


Figure 5: The spectrum of the discrete approximation to (15) multiplied by h_R for the sixth-order discretization, with the characteristic coupling (left) and quadratic coupling (right). 21^2 unknowns in the left (coarse) block.)

II Parabolic problems

In this section we extend the analysis to include parabolic problems (such as Navier-Stokes equations) of the form

$$\begin{aligned} \mathbf{u}_t + A\mathbf{u}_x + B\mathbf{u}_y &= C_{11}\mathbf{u}_{xx} + C_{12}\mathbf{u}_{xy} + C_{21}\mathbf{u}_{yx} + C_{22}\mathbf{u}_{yy}, \quad \mathbf{x} \in \Omega_{d,u}^{l,i}, \\ \mathbf{v}_t + A\mathbf{v}_x + B\mathbf{v}_y &= C_{11}\mathbf{v}_{xx} + C_{12}\mathbf{v}_{xy} + C_{21}\mathbf{v}_{yx} + C_{22}\mathbf{v}_{yy}, \quad \mathbf{x} \in \Omega_{d,u}^{i,r}, \end{aligned} \quad (17)$$

where A and B are symmetric $k \times k$ matrices. The continuity conditions at the interface are given by: $u = v, u_x = v_x, u_y = v_y$. Parabolicity requires that,

$$x^T(C + C^T)x \geq 0, \quad (18)$$

where

$$C = \begin{bmatrix} C_{11} & C_{12} \\ C_{21} & C_{22} \end{bmatrix}.$$

A corresponding semi-discrete approximation of (17) can be written

$$\begin{aligned} u_t + A \otimes \mathbf{D}_L^x u + B \otimes \mathbf{D}_L^y u &= P_L + SAT_{IL}^I + SAT_{IL}^V + SAT_L^V \\ v_t + A \otimes \mathbf{D}_R^x v + B \otimes \mathbf{D}_R^y v &= P_R + SAT_{IR}^I + SAT_{IR}^V + SAT_R^V, \end{aligned} \quad (19)$$

where

$$\begin{aligned} P_L &= C_{11} \otimes \mathbf{D}_L^x \mathbf{D}_L^x u + C_{12} \otimes \mathbf{D}_L^x \mathbf{D}_L^y u + C_{21} \otimes \mathbf{D}_L^y \mathbf{D}_L^x u + C_{22} \otimes \mathbf{D}_L^y \mathbf{D}_L^y u \\ P_R &= C_{11} \otimes \mathbf{D}_R^x \mathbf{D}_R^x v + C_{12} \otimes \mathbf{D}_R^x \mathbf{D}_R^y v + C_{21} \otimes \mathbf{D}_R^y \mathbf{D}_R^x v + C_{22} \otimes \mathbf{D}_R^y \mathbf{D}_R^y v, \end{aligned}$$

$$\begin{aligned}
SAT_{IL}^V &= \Sigma_L^2 C_{11} \otimes (\mathbf{H}_L^x)^{-1} (\mathbf{D}_L^x)^T \mathbf{e}_N^x \{u_N - I_k \otimes I_{F2C} v_0\} \\
&\quad C_{11} \Sigma_L^3 \otimes (\mathbf{H}_L^x)^{-1} \mathbf{e}_N^x \{(I_k \otimes \mathbf{D}_L^x u)_N - I_k \otimes I_{F2C} (I_k \otimes \mathbf{D}_R^x v)_0\} \\
&\quad \Sigma_L^4 C_{21} \otimes (\mathbf{H}_L^x)^{-1} (\mathbf{D}_L^y)^T \mathbf{e}_N^x \{u_N - I_k \otimes I_{F2C} v_0\} \\
&\quad C_{21} \Sigma_L^5 \otimes (\mathbf{H}_L^x)^{-1} \mathbf{e}_N^x \{(I_k \otimes \mathbf{D}_L^y u)_N - I_k \otimes I_{F2C} (I_k \otimes \mathbf{D}_R^y v)_0\} , \\
SAT_{IR}^V &= \Sigma_R^2 C_{11} \otimes (\mathbf{H}_R^x)^{-1} (\mathbf{D}_R^x)^T \mathbf{e}_0^x \{v_0 - I_k \otimes I_{C2F} u_N\} \\
&\quad C_{11} \Sigma_R^3 \otimes (\mathbf{H}_R^x)^{-1} \mathbf{e}_N^x \{(I_k \otimes \mathbf{D}_R^x v)_0 - I_k \otimes I_{C2F} (I_k \otimes \mathbf{D}_L^x u)_N\} \\
&\quad \Sigma_R^4 C_{21} \otimes (\mathbf{H}_R^x)^{-1} (\mathbf{D}_R^y)^T \mathbf{e}_0^x \{v_0 - I_k \otimes I_{C2F} u_N\} \\
&\quad C_{21} \Sigma_R^5 \otimes (\mathbf{H}_R^x)^{-1} \mathbf{e}_N^x \{(I_k \otimes \mathbf{D}_R^y v)_0 - I_k \otimes I_{C2F} (I_k \otimes \mathbf{D}_L^y u)_N\} ,
\end{aligned}$$

SAT_{IL}^I and SAT_{IR}^I are given by Eq. (7), or Eq. (14). SAT_{IL}^V and SAT_{IR}^V are the SAT penalty terms handling the viscous multi-block coupling. $SAT_{L,R}^V$ denote the viscous penalty terms at the outer boundaries. (These are tuned to obtain stability, see [24, 22, 35] for details.)

Lemma II.1 *The scheme (19) is stable if*

$$\begin{aligned}
\Sigma_R^2 &= \Sigma^2, \quad \Sigma_L^2 = \Sigma^2 - I, \quad \Sigma_L^3 = -\Sigma^2, \quad \Sigma_R^3 = I - \Sigma^2, \\
\Sigma_R^4 &= \Sigma^4, \quad \Sigma_L^4 = \Sigma^4 - I, \quad \Sigma_L^5 = -\Sigma^4, \quad \Sigma_R^5 = I - \Sigma^4,
\end{aligned}$$

and Lemma 3.2, Lemma 3.3 or Lemma 3.4 hold, assuming that the boundary terms $SAT_{L,R}^V$ are correctly implemented. $\Sigma^{2,4}$ are symmetric matrices.

Proof Apply the energy method by multiplying the first and second equation in (19) by $u^T M_L$ and $v^T M_R$ (defined by (8)) respectively, yielding,

$$\frac{d}{dt} (\|u\|_{M_L} + \|v\|_{M_R}) = BT^V + IT^I + IT^V + (IT^V)^T.$$

BT^V corresponds to the outer boundary terms (which we assume are correctly implemented, i.e., bounded). IT^I is given by (9) and corresponds to the inviscid part. $IT^V + (IT^V)^T$ correspond to the viscous part of the multi-block coupling given by:

$$\begin{aligned}
&+ u_N^T C_{11} (I_k + \Sigma_L^2 + \Sigma_L^3) (H_L^y \otimes \mathbf{D}_L^x u)_N \\
&- u_N^T C_{11} \otimes I^y (\Sigma_L^3 \otimes H_L^y + \Sigma_R^2 \otimes I_{C2F}^T H_R^y) (I_k \otimes \mathbf{D}_R^x v)_0 \\
&- v_0^T C_{11} (I_k - \Sigma_R^2 - \Sigma_R^3) (H_R^y \otimes \mathbf{D}_R^x v)_0 \\
&- v_0^T C_{11} \otimes I^y (\Sigma_R^3 \otimes H_R^y + \Sigma_L^2 \otimes I_{F2C}^T H_L^y) (I_k \otimes \mathbf{D}_L^x u)_N \\
IT^V &= + u_N^T C_{21} (I_k + \Sigma_L^4 + \Sigma_L^5) (H_L^y \otimes \mathbf{D}_L^y u)_N \\
&- u_N^T C_{21} \otimes I^y (\Sigma_L^5 \otimes H_L^y + \Sigma_R^4 \otimes I_{C2F}^T H_R^y) (I_k \otimes \mathbf{D}_R^y v)_0 \\
&- v_0^T C_{21} (I_k - \Sigma_R^4 - \Sigma_R^5) (H_R^y \otimes \mathbf{D}_R^y v)_0 \\
&- v_0^T C_{21} \otimes I^y (\Sigma_R^5 \otimes H_R^y + \Sigma_L^4 \otimes I_{F2C}^T H_L^y) (I_k \otimes \mathbf{D}_L^y u)_N.
\end{aligned}$$

A stable coupling is obtained if IT^I is non-positive and if IT^V vanish. By assumption Lemma 3.2, Lemma 3.3 or Lemma 3.4 hold which means that IT^I is non-positive. By choosing:

$$\begin{aligned}\Sigma_R^2 &= \Sigma^2, \quad \Sigma_L^2 = \Sigma^2 - I_k, \quad \Sigma_L^3 = -\Sigma^2, \quad \Sigma_R^3 = I_k - \Sigma^2, \\ \Sigma_R^4 &= \Sigma^4, \quad \Sigma_L^4 = \Sigma^4 - I_k, \quad \Sigma_L^5 = -\Sigma^4, \quad \Sigma_R^5 = I_k - \Sigma^4,\end{aligned}$$

(in combination with (11)) $IT^V = 0$. \square

Remark The symmetric matrices Σ^2 and Σ^4 can be chosen arbitrarily for stability. (Note that Σ^2, Σ^4 are not powers of Σ , but different parameters). However, the specific choice will affect the eigenvalues of (19). We use $\Sigma^2 = \Sigma^4 = I_k/2$ since it leads to a compact spectrum (we have no proof that this particular choice is optimal).

III Interpolation Operators

III.1 Second-Order case

The discrete norm is given by $H = h \text{diag}(\frac{1}{2}, 1, \dots, 1, \frac{1}{2})$. The interpolation operators are given by:

$$I_{F2C} = \begin{bmatrix} \frac{11}{20} & \frac{1}{2} & -\frac{1}{20} & & & & & & \\ -\frac{1}{40} & \frac{1}{4} & \frac{11}{20} & \frac{1}{4} & -\frac{1}{40} & & & & \\ & & -\frac{1}{40} & \frac{1}{4} & \frac{11}{20} & \frac{1}{4} & -\frac{1}{40} & & \\ & & & \ddots & \ddots & \ddots & \ddots & \ddots & \\ & & & & -\frac{1}{40} & \frac{1}{4} & \frac{11}{20} & \frac{1}{4} & -\frac{1}{40} \\ & & & & & -\frac{1}{40} & \frac{1}{4} & \frac{11}{20} & \frac{1}{4} & -\frac{1}{40} \\ & & & & & & -\frac{1}{20} & \frac{1}{2} & \frac{11}{20} & \end{bmatrix}$$

and

$$I_{C2F} = \begin{bmatrix} \frac{11}{10} & -\frac{1}{10} & & & & & & & \\ & \frac{1}{2} & \frac{1}{2} & & & & & & \\ & -\frac{1}{20} & \frac{11}{10} & -\frac{1}{20} & & & & & \\ & & \frac{1}{2} & \frac{1}{2} & & & & & \\ & & -\frac{1}{20} & \frac{11}{10} & -\frac{1}{20} & & & & \\ & & & \frac{1}{2} & \frac{1}{2} & & & & \\ & & & -\frac{1}{20} & \frac{11}{10} & -\frac{1}{20} & & & \\ & & & & \ddots & \ddots & \ddots & & \\ & & & & & -\frac{1}{20} & \frac{11}{10} & -\frac{1}{20} \\ & & & & & & \frac{1}{2} & \frac{1}{2} \\ & & & & & & -\frac{1}{10} & \frac{11}{10} \end{bmatrix}$$

III.2 Fourth- to Second-Order Case

Fourth to second-order, with second-order accurate interpolation. The upper left corner of I_{F2C} is given by:

$$\begin{aligned} a_{1,1} &= \frac{198814379483797276626589}{292154366866608903386020} & a_{2,1} &= \frac{1342353899420590372183}{101394750853705442939854} & a_{3,1} &= -\frac{6011306572161601487699}{738978692662598990917580} \\ a_{1,2} &= \frac{33159311983113441321394}{73038591716652225846505} & a_{2,2} &= \frac{87193543695192148191232}{253486877134263607349635} & a_{3,2} &= -\frac{17239549725384800082266}{184744673165649747729395} \\ a_{1,3} &= \frac{1971623072622604595228923}{16828091531516672835034752} & a_{2,3} &= \frac{5578077558511726076198789}{19467792163911445044451968} & a_{3,3} &= \frac{13200899856172905887766503}{70941954495609503128087680} \\ a_{1,4} &= -\frac{95808836247685639307767}{824906447623366315442880} & a_{2,4} &= \frac{3895790315853711272834919}{16223160136592870870376640} & a_{3,4} &= \frac{3693069541319881367608217}{11823659082601583854681280} \\ a_{1,5} &= -\frac{1754070195140572218604399}{10517557207197920521896720} & a_{2,5} &= \frac{2244981324267232772622413}{12167370102444653152782480} & a_{3,5} &= \frac{1607455065911582798562599}{8867744311951187891010960} \\ a_{1,6} &= -\frac{237072760963890638174137}{14023409609597227362528960} & a_{2,6} &= -\frac{213524706698808911938359}{16223160136592870870376640} & a_{3,6} &= \frac{3514316393052784877273751}{11823659082601583854681280} \\ a_{1,7} &= \frac{55326079761477589117471}{2804681921919445472505792} & a_{2,7} &= -\frac{2744378984383218872921257}{48669480409778612611129920} & a_{3,7} &= \frac{8869555969232379886041937}{35470977247804751564043840} \\ a_{1,8} &= -\frac{120787724660864994449209}{14023409609597227362528960} & a_{2,8} &= \frac{177648545875941908529241}{16223160136592870870376640} & a_{3,8} &= -\frac{652819712407377597489161}{11823659082601583854681280} \\ a_{1,9} &= \frac{176943055421257964368859}{10517557207197920521896720} & a_{2,9} &= -\frac{45572983468520710671107}{12167370102444653152782480} & a_{3,9} &= -\frac{129041283038038640595559}{1773548862390237578202192} \\ a_{1,10} &= \frac{32831043571234596789193}{14023409609597227362528960} & a_{2,10} &= \frac{3876549717482752134187}{3244632027318574174075328} & a_{3,10} &= -\frac{21210275952319643393399}{11823659082601583854681280} \\ a_{1,11} &= \frac{88481545475605230181351}{4949438685740197892657280} & a_{2,11} &= -\frac{704697674731763751811223}{9733896081955722522259840} & a_{3,11} &= \frac{300890344598183653971671}{70941954495609503128087680} \end{aligned}$$

The interior of I_{F2C} is given by:

$$\begin{aligned} a_4 &= -\frac{292764282684548619564311}{4949438685740197892657280} & a_1 &= \frac{233575073382358527482521}{824906447623366315442880} \\ a_3 &= -\frac{27348461476516948621801}{824906447623366315442880} & a_0 &= \frac{139882799512953873064261}{824906447623366315442880} \\ a_2 &= \frac{138809444447592059191981}{618679835717524736582160} \end{aligned}$$

The upper left corner of I_{C2F} is given by:

$$\begin{aligned}
b_{1,1} &= \frac{198814379483797276626589}{206226611905841578860720} & b_{6,1} &= -\frac{237072760963890638174137}{19797754742960791570629120} & b_{9,4} &= \frac{6801662777932010900407069}{14848316057220593677971840} \\
b_{1,2} &= \frac{1342353899420590372183}{20622661190584157886072} & b_{6,2} &= -\frac{71174902232936303979453}{2199750526995643507847680} & b_{9,5} &= \frac{139882799512953873064261}{412453223811683157721440} \\
b_{1,3} &= -\frac{6011306572161601487699}{206226611905841578860720} & b_{6,3} &= \frac{1171438797684261625757917}{2199750526995643507847680} & b_{9,6} &= \frac{138809444447592059191981}{309339917858762368291080} \\
b_{2,1} &= \frac{16579655991556720660697}{51556652976460394715180} & b_{6,4} &= \frac{11445178595735567846643529}{19797754742960791570629120} & b_{9,7} &= -\frac{292764282684548619564311}{2474719342870098946328640} \\
b_{2,2} &= \frac{10899192961899018523904}{12889163244115098678795} & b_{6,5} &= -\frac{27348461476516948621801}{412453223811683157721440} & b_{10,1} &= \frac{32831043571234596789193}{19797754742960791570629120} \\
b_{2,3} &= -\frac{8619774862692400041133}{51556652976460394715180} & b_{7,1} &= \frac{55326079761477589117471}{3959550948592158314125824} & b_{10,2} &= \frac{3876549717482752134187}{1319850316197386104708608} \\
b_{3,1} &= \frac{1971623072622604595228923}{23757305691552949884754944} & b_{7,2} &= -\frac{2744378984383218872921257}{19797754742960791570629120} & b_{10,3} &= -\frac{21210275952319643393399}{6599251580986930523543040} \\
b_{3,2} &= \frac{5578077558511726076198789}{7919101897184316628251648} & b_{7,3} &= \frac{8869555969232379886041937}{19797754742960791570629120} & b_{10,4} &= -\frac{1340074612349330482468249}{19797754742960791570629120} \\
b_{3,3} &= \frac{13200899856172905887766503}{39595509485921583141258240} & b_{7,4} &= \frac{6854257176134739780148789}{19797754742960791570629120} & b_{10,5} &= \frac{233575073382358527482521}{412453223811683157721440} \\
b_{3,4} &= -\frac{14345449851542882358651239}{118786528457764749423774720} & b_{7,5} &= \frac{138809444447592059191981}{309339917858762368291080} & b_{10,6} &= \frac{412453223811683157721440}{412453223811683157721440} \\
b_{4,1} &= -\frac{1628750216210655868232039}{19797754742960791570629120} & b_{7,6} &= -\frac{292764282684548619564311}{2474719342870098946328640} & b_{10,7} &= -\frac{27348461476516948621801}{412453223811683157721440} \\
b_{4,2} &= \frac{1298596771951237090944973}{2199750526995643507847680} & b_{8,1} &= -\frac{120787724660864994449209}{19797754742960791570629120} & b_{11,1} &= \frac{1504186273085288913082967}{118786528457764749423774720} \\
b_{4,3} &= \frac{3693069541319881367608217}{6599251580986930523543040} & b_{8,2} &= \frac{177648545875941908529241}{6599251580986930523543040} & b_{11,2} &= -\frac{704697674731763751811223}{39595509485921583141258240} \\
b_{4,4} &= -\frac{1340074612349330482468249}{19797754742960791570629120} & b_{8,3} &= -\frac{652819712407377597489161}{6599251580986930523543040} & b_{11,3} &= \frac{300890344598183653971671}{39595509485921583141258240} \\
b_{5,1} &= -\frac{1754070195140572218604399}{14848316057220593677971840} & b_{8,4} &= \frac{11445178595735567846643529}{19797754742960791570629120} & b_{11,4} &= -\frac{14345449851542882358651239}{118786528457764749423774720} \\
b_{5,2} &= \frac{2244981324267232772622413}{4949438685740197892657280} & b_{8,5} &= \frac{233575073382358527482521}{412453223811683157721440} & b_{11,5} &= \frac{138809444447592059191981}{309339917858762368291080} \\
b_{5,3} &= \frac{1607455065911582798562599}{4949438685740197892657280} & b_{8,6} &= -\frac{27348461476516948621801}{412453223811683157721440} & b_{11,6} &= \frac{139882799512953873064261}{412453223811683157721440} \\
b_{5,4} &= \frac{6801662777932010900407069}{14848316057220593677971840} & b_{9,1} &= \frac{176943055421257964368859}{14848316057220593677971840} & b_{11,7} &= \frac{138809444447592059191981}{309339917858762368291080} \\
b_{5,5} &= -\frac{292764282684548619564311}{2474719342870098946328640} & b_{9,2} &= -\frac{45572983468520710671107}{4949438685740197892657280} & b_{11,8} &= -\frac{292764282684548619564311}{2474719342870098946328640} \\
b_{9,3} &= -\frac{129041283038038640595559}{989887737148039578531456} & & & &
\end{aligned}$$

III.3 Fourth-Order Case

The discrete norm is given by $H = h \text{diag}(\frac{17}{48}, \frac{59}{48}, \frac{43}{48}, \frac{49}{48}, 1, \dots)$.

The upper left corner of I_{F2C} is given by:

$$\begin{array}{lll}
a_{1,1} = \frac{37625155150141581259}{74136705821905530032} & a_{2,1} = -\frac{9465638066209876131}{2187032821746213135944} & a_{3,1} = \frac{9465638066209876131}{3187878350341937791376} \\
a_{1,2} = \frac{109494000531368265009}{157540499871549251318} & a_{2,2} = \frac{6477310271684014677}{18534176455476382508} & a_{3,2} = -\frac{54391101655540111975}{796969587585484447844} \\
a_{1,3} = \frac{598984862036951996355}{20165183983558304168704} & a_{2,3} = \frac{23789903736542318389255}{69985050295878820350208} & a_{3,3} = \frac{1629291546275511894441}{51006053605471004662016} \\
a_{1,4} = -\frac{259928664916563226325}{2520647997944788021088} & a_{2,4} = \frac{2109162960890226252711}{8748131286984852543776} & a_{3,4} = \frac{2010507950879293630905}{6375756700683875582752} \\
a_{1,5} = -\frac{256587334010286818055}{5041295995889576042176} & a_{2,5} = \frac{776008005836532793785}{17496262573969705087552} & a_{3,5} = \frac{6208709747109065353983}{12751513401367751165504} \\
a_{1,6} = -\frac{113845943840605140771}{2520647997944788021088} & a_{2,6} = \frac{46983667240315552089}{8748131286984852543776} & a_{3,6} = \frac{1804441319301200448807}{6375756700683875582752} \\
a_{1,7} = -\frac{537477213186037277591}{10082591991779152084352} & a_{2,7} = \frac{1087641244818460785021}{34992525147939410175104} & a_{3,7} = -\frac{58210841472168154533}{25503026802735502331008} \\
a_{1,8} = -\frac{89579548577713740579}{2520647997944788021088} & a_{2,8} = \frac{220860994180249341801}{8748131286984852543776} & a_{3,8} = -\frac{395393460093074051961}{6375756700683875582752} \\
a_{1,9} = -\frac{33361750807060821603}{5041295995889576042176} & a_{2,9} = \frac{77236835126760009513}{17496262573969705087552} & a_{3,9} = -\frac{180548419983997949901}{12751513401367751165504} \\
a_{1,10} = \frac{45876275221828488395}{2520647997944788021088} & a_{2,10} = -\frac{96386094557526072417}{8748131286984852543776} & a_{3,10} = \frac{55143363449566679649}{6375756700683875582752} \\
a_{1,11} = \frac{891498675213598216803}{20165183983558304168704} & a_{2,11} = -\frac{1793510683939834799913}{69985050295878820350208} & a_{3,11} = \frac{21221519586950580219}{1186187293150488480512}
\end{array}$$

The interior stencil is given by:

$$\begin{array}{lll}
a_4 = -\frac{10513333512638366307}{1186187293150488480512} & a_2 = \frac{10513333512638366307}{296546823287622120128} & a_1 = \frac{9}{32} \\
a_3 = -\frac{1}{32} & & a_0 = \frac{265006822749707021207}{593093646575244240256}
\end{array}$$

The upper left part of I_{C2F} is given by:

$$\begin{aligned}
b_{1,1} &= \frac{37625155150141581259}{37068352910952765016} & b_{6,1} &= -\frac{37948647946868380257}{1186187293150488480512} & b_{9,3} &= -\frac{60182806661332649967}{2372374586300976961024} \\
b_{1,2} &= -\frac{556802239188816243}{18534176455476382508} & b_{6,2} &= \frac{1566122413438517363}{1186187293150488480512} & b_{9,4} &= \frac{171717780706426649681}{2372374586300976961024} \\
b_{1,3} &= \frac{556802239188816243}{37068352910952765016} & b_{6,2} &= \frac{601480439767066816269}{1186187293150488480512} & b_{9,5} &= \frac{265006822749707021207}{296546823287622120128} \\
b_{2,1} &= \frac{1855830517480818051}{4633544113869095627} & b_{6,2} &= \frac{147}{256} & b_{9,6} &= \frac{10513333512638366307}{148273411643811060064} \\
b_{2,2} &= \frac{6477310271684014677}{9267088227738191254} & b_{6,2} &= -\frac{1}{16} & b_{9,7} &= -\frac{10513333512638366307}{593093646575244240256} \\
b_{2,3} &= -\frac{921883078907459525}{9267088227738191254} & b_{7,1} &= -\frac{537477213186037277591}{14234247517805861766144} & b_{10,1} &= \frac{45876275221828488395}{3558561879451465441536} \\
b_{3,1} &= \frac{598984862036951996355}{25503026802735502331008} & b_{7,2} &= \frac{362547081606153595007}{4744749172601953922048} & b_{10,2} &= -\frac{32128698185842024139}{1186187293150488480512} \\
b_{3,2} &= \frac{23789903736542318389255}{25503026802735502331008} & b_{7,3} &= -\frac{19403613824056051511}{4744749172601953922048} & b_{10,3} &= \frac{18381121149855559883}{1186187293150488480512} \\
b_{3,3} &= \frac{1629291546275511894441}{25503026802735502331008} & b_{7,4} &= \frac{12985334314735644039143}{14234247517805861766144} & b_{10,4} &= -\frac{49}{768} \\
b_{3,4} &= -\frac{515153342119279949043}{25503026802735502331008} & b_{7,5} &= \frac{10513333512638366307}{148273411643811060064} & b_{10,5} &= \frac{9}{16} \\
b_{4,1} &= -\frac{5304666630950269925}{74136705821905530032} & b_{7,6} &= -\frac{10513333512638366307}{593093646575244240256} & b_{10,6} &= \frac{9}{16} \\
b_{4,2} &= \frac{43044142058984209239}{74136705821905530032} & b_{8,1} &= -\frac{29859849525904580193}{1186187293150488480512} & b_{10,7} &= -\frac{1}{16} \\
b_{4,3} &= \frac{41030774507740686345}{74136705821905530032} & b_{8,2} &= \frac{73620331393416447267}{1186187293150488480512} & b_{11,1} &= \frac{297166225071199405601}{9489498345203907844096} \\
b_{4,4} &= -\frac{1}{16} & b_{8,3} &= -\frac{131797820031024683987}{1186187293150488480512} & b_{11,2} &= -\frac{597836894646611599971}{9489498345203907844096} \\
b_{5,1} &= -\frac{85529111336762272685}{2372374586300976961024} & b_{8,4} &= \frac{147}{256} & b_{11,3} &= \frac{304175114079624983139}{9489498345203907844096} \\
b_{5,2} &= \frac{258669335278844264595}{2372374586300976961024} & b_{8,5} &= \frac{9}{16} & b_{11,4} &= -\frac{171717780706426649681}{9489498345203907844096} \\
b_{5,2} &= \frac{2069569915703021784661}{2372374586300976961024} & b_{8,6} &= -\frac{1}{16} & b_{11,5} &= \frac{10513333512638366307}{148273411643811060064} \\
b_{5,2} &= \frac{171717780706426649681}{2372374586300976961024} & b_{9,1} &= -\frac{11120583602353607201}{2372374586300976961024} & b_{11,6} &= \frac{265006822749707021207}{296546823287622120128} \\
b_{5,2} &= -\frac{10513333512638366307}{593093646575244240256} & b_{9,2} &= \frac{25745611708920003171}{2372374586300976961024} & b_{11,7} &= \frac{10513333512638366307}{148273411643811060064} \\
& & & & b_{11,8} &= -\frac{10513333512638366307}{593093646575244240256}
\end{aligned}$$

III.4 Fourth-Order Case, Non-SBP Interpolation

The upper left part of I_{C2F} :

$$\begin{pmatrix}
1 & & & & & & & & \\
\frac{5}{16} & \frac{15}{16} & -\frac{5}{16} & \frac{1}{16} & & & & & \\
& 1 & & & & & & & \\
2a_3 & 2a_1 & 2a_1 & 2a_3 & & & & & \\
2a_4 & 2a_2 & 2a_0 & 2a_2 & 2a_4 & & & & \\
& & 2a_3 & 2a_1 & 2a_1 & 2a_3 & & & \\
& & 2a_4 & 2a_2 & 2a_0 & 2a_2 & 2a_4 & & \\
& & & \ddots & \ddots & \ddots & & &
\end{pmatrix}$$

The lower left part of I_{F2C} :

$$\begin{pmatrix} 1 & & & & & & & & & & \\ & 1 & & & & & & & & & \\ & a_4 & a_3 & a_2 & a_1 & a_0 & a_1 & a_2 & a_3 & a_4 & \\ & & & a_4 & a_3 & a_2 & a_1 & a_0 & a_1 & a_2 & a_3 & a_4 \\ & & & & \ddots & \ddots & \ddots & \ddots & \ddots & \ddots & \ddots & \ddots \end{pmatrix}$$

a_{0-4} is listed in previous subsection.

III.5 Sixth-Order Case

Sixth order accurate case is given below. Notice that the stability condition for the upwind formulation could not be achieved. The discrete norm is given by $H = h \text{diag}(\frac{13649}{43200}, \frac{12013}{8640}, \frac{2711}{4320}, \frac{5359}{4320}, \frac{7877}{8640}, \frac{43801}{43200}, 1, \dots)$.

The upper left corner of I_{F2C} is given by:

$$\begin{aligned}
a_{1,1} &= \frac{493203253466037198549455362364169948587300751}{1055237669662369450269932613530339432431112782} & a_{2,9} &= -\frac{37294205185814962316045245318486095186507918}{464377248357170642761107058624806491383799467} \\
a_{1,2} &= \frac{2802735}{3494144} & a_{2,10} &= -\frac{100125}{768832} \\
a_{1,3} &= \frac{65307081693884397225173945017702348750445730}{527618834831184725134966306765169716215556391} & a_{2,11} &= -\frac{36281493221658864449474225976906916398553827}{928754496714341285522214117249612982767598934} \\
a_{1,4} &= -\frac{729595}{6988288} & a_{2,12} &= \frac{55219}{768832} \\
a_{1,5} &= -\frac{114866096841096884636391939697630554903763548}{527618834831184725134966306765169716215556391} & a_{2,13} &= \frac{22445907670907889073586224542480749734259694}{464377248357170642761107058624806491383799467} \\
a_{1,6} &= -\frac{1668147}{6988288} & a_{2,14} &= -\frac{63387}{6150656} \\
a_{1,7} &= -\frac{58150488726161516985950806005548507936924127}{527618834831184725134966306765169716215556391} & a_{2,15} &= -\frac{5433667362017414115320173550603825973179156}{464377248357170642761107058624806491383799467} \\
a_{1,8} &= \frac{15525}{436768} & a_{2,16} &= \frac{5409}{6150656} \\
a_{1,9} &= \frac{160596781068985961753206980048680817748946115}{1055237669662369450269932613530339432431112782} & a_{2,17} &= \frac{578944702382543295705133726021669910745894}{464377248357170642761107058624806491383799467} \\
a_{1,10} &= \frac{89725}{436768} & a_{3,1} &= -\frac{5162337204772128987826641660149965144238346}{104797029908956098603626174638462532102012849} \\
a_{1,11} &= \frac{28603010322006197876985672016642805153037153}{527618834831184725134966306765169716215556391} & a_{3,2} &= -\frac{240439}{1388032} \\
a_{1,12} &= -\frac{858195}{6988288} & a_{3,3} &= \frac{23386090748321137420688072323840400038565838}{104797029908956098603626174638462532102012849} \\
a_{1,13} &= -\frac{42754568564745224527531090194001857246708700}{527618834831184725134966306765169716215556391} & a_{3,4} &= \frac{105687}{173504} \\
a_{1,14} &= \frac{124485}{6988288} & a_{3,5} &= \frac{120607102321976279545796687898247496534070403}{419188119635824394414504698553850128408051396} \\
a_{1,15} &= \frac{10622334830569558938004175701898426132770338}{527618834831184725134966306765169716215556391} & a_{3,6} &= \frac{75135}{694016} \\
a_{1,16} &= -\frac{5409}{3494144} & a_{3,7} &= -\frac{14476182846428389369733457155565337017487527}{209594059817912197207252349276925064204025698} \\
a_{1,17} &= -\frac{1157889404765086591410267452043339821491788}{527618834831184725134966306765169716215556391} & a_{3,8} &= -\frac{217175}{1388032} \\
a_{2,1} &= \frac{10324674409544257975653283320299930288476692}{464377248357170642761107058624806491383799467} & a_{3,9} &= \frac{6622670052963322216326122365241056731782031}{209594059817912197207252349276925064204025698} \\
a_{2,2} &= \frac{1201479}{3075328} & a_{3,10} &= \frac{344085}{1388032} \\
a_{2,3} &= \frac{63083470065854914766431215082154659242790665}{464377248357170642761107058624806491383799467} & a_{3,11} &= \frac{21321625226448423053859202901015977066304133}{209594059817912197207252349276925064204025698} \\
a_{2,4} &= \frac{721527}{3075328} & a_{3,12} &= -\frac{78363}{694016} \\
a_{2,5} &= \frac{75656801964097450751057400512505712346209266}{464377248357170642761107058624806491383799467} & a_{3,13} &= -\frac{8305592718705970541713249560330845208737268}{104797029908956098603626174638462532102012849} \\
a_{2,6} &= \frac{838645}{6150656} & a_{3,14} &= \frac{5473}{347008} \\
a_{2,7} &= \frac{30937093119827557151778923229206427591240999}{464377248357170642761107058624806491383799467} & a_{3,15} &= \frac{1892889085160894469318781649971017262255710}{104797029908956098603626174638462532102012849} \\
a_{2,8} &= \frac{345}{6150656} & a_{3,16} &= -\frac{1803}{1388032} \\
& & a_{3,17} &= -\frac{192981567460847765235044575340556636915298}{104797029908956098603626174638462532102012849}
\end{aligned}$$

The interior of I_{F2C} is given by:

$$\begin{aligned}
a_6 &= \frac{321100777805071156797079160300427016498}{38656226451108852306759931626138890483959} & a_2 &= \frac{4816511667076067351956187404506405247470}{38656226451108852306759931626138890483959} \\
a_5 &= \frac{3}{512} & a_1 &= \frac{75}{256} \\
a_4 &= -\frac{1926604666830426940782474961802562098988}{38656226451108852306759931626138890483959} & a_0 &= \frac{25812195338906006034876765214121809824039}{77312452902217704613519863252277780967918} \\
a_3 &= -\frac{25}{512}
\end{aligned}$$

III.6 Sixth-Order Case, Non-SBP Interpolation

The upper left part of I_{C2F} :

$$\left(\begin{array}{cccccc} 1 & & & & & \\ \frac{63}{256} & \frac{315}{256} & -\frac{105}{128} & \frac{63}{128} & -\frac{45}{256} & \frac{7}{256} \\ & 1 & & & & \\ -\frac{7}{256} & \frac{105}{256} & \frac{105}{128} & -\frac{35}{128} & \frac{21}{256} & -\frac{3}{256} \\ & & 1 & & & \\ 2a_5 & 2a_3 & 2a_1 & 2a_1 & 2a_3 & 2a_5 \\ 2a_6 & 2a_4 & 2a_2 & 2a_0 & 2a_2 & 2a_4 & 2a_6 \\ & & 2a_5 & 2a_3 & 2a_1 & 2a_1 & 2a_3 & 2a_5 \\ & & 2a_6 & 2a_4 & 2a_2 & 2a_0 & 2a_2 & 2a_4 & 2a_6 \\ & & & \ddots & \ddots & \ddots & \ddots & \ddots & \ddots \end{array} \right)$$

The lower left part of I_{F2C} :

[illegible]

a_{0-6} is listed in previous subsection.

III.7 Eighth-Order Case

The upper left corner of I_{F2C} is given by:

| | | |
|---|--|--|
| $a_{1,1} = 0.49670323986410765203$ | $a_{2,8} = 0.65828018436035862232$ | $a_{3,16} = 1.9882413967858906122$ |
| $a_{1,2} = 0.80670591743192512511$ | $a_{2,9} = 0.039704539050575728856$ | $a_{3,17} = 1.7259601262271516763$ |
| $a_{1,3} = -0.014476656476698073533$ | $a_{2,10} = -0.47252462545568042557$ | $a_{3,18} = -0.36895458453625989435$ |
| $a_{1,4} = -0.19497555250083395132$ | $a_{2,11} = -0.44892698918501097924$ | $a_{3,19} = -0.50448363278283993228$ |
| $a_{1,5} = 0.16074268813765884450$ | $a_{2,12} = -0.34402935194949605213$ | $a_{3,20} = 0.052797763052066775846$ |
| $a_{1,6} = 0.22100911221277072755$ | $a_{2,13} = 0.087284452472801643396$ | $a_{3,21} = 0.088972343374038343284$ |
| $a_{1,7} = -0.53042418939472250452$ | $a_{2,14} = 0.59539401290875351190$ | $a_{3,22} = -0.0037175165926095403240$ |
| $a_{1,8} = -0.86254139670456354517$ | $a_{2,15} = 0.30484430526276345964$ | $a_{3,23} = -0.0071737841052106668688$ |
| $a_{1,9} = 0.0064231825172866668299$ | $a_{2,16} = -0.27096308216867871783$ | $a_{4,1} = 0.0021626748627943672418$ |
| $a_{1,10} = 0.69727164011248914487$ | $a_{2,17} = -0.23108785344796321535$ | $a_{4,2} = 0.027636709246281031633$ |
| $a_{1,11} = 0.61825742343094006838$ | $a_{2,18} = 0.050608234918774219796$ | $a_{4,3} = -0.00055259484658035070394$ |
| $a_{1,12} = 0.43307239695721032895$ | $a_{2,19} = 0.068801842319351676214$ | $a_{4,4} = -0.033553649469391355855$ |
| $a_{1,13} = -0.15848187861199173328$ | $a_{2,20} = -0.0073322707316320135247$ | $a_{4,5} = -0.049244245327794891233$ |
| $a_{1,14} = -0.83836831742920925562$ | $a_{2,21} = -0.012333488857215226757$ | $a_{4,6} = 0.093489376222103426899$ |
| $a_{1,15} = -0.41767239062238727391$ | $a_{2,22} = 0.00052275043402033040521$ | $a_{4,7} = 0.45734620580442859300$ |
| $a_{1,16} = 0.39252899650233765024$ | $a_{2,23} = 0.0010087644967132781708$ | $a_{4,8} = 0.665796091523388478842$ |
| $a_{1,17} = 0.33094736964907844809$ | $a_{3,1} = -0.022656973277393401539$ | $a_{4,9} = 0.24716623315221892947$ |
| $a_{1,18} = -0.073592865087013788440$ | $a_{3,2} = -0.93771184228725468159$ | $a_{4,10} = -0.15893464065423852815$ |
| $a_{1,19} = -0.099669762780958210515$ | $a_{3,3} = -0.052699680965389826267$ | $a_{4,11} = -0.25881084331023040874$ |
| $a_{1,20} = 0.010748160731101219580$ | $a_{3,4} = 1.9581430555012001670$ | $a_{4,12} = -0.26865808253702445366$ |
| $a_{1,21} = 0.018056833808814782786$ | $a_{3,5} = 1.6586148101136731602$ | $a_{4,13} = -0.018060020510041282529$ |
| $a_{1,22} = -0.00077275234787125894193$ | $a_{3,6} = 2.7435837109255836264$ | $a_{4,14} = 0.30841043055726240020$ |
| $a_{1,23} = -0.0014911993994710636483$ | $a_{3,7} = -3.0164708462284474624$ | $a_{4,15} = 0.17712461121229459766$ |
| $a_{2,1} = 0.0025487859584304862664$ | $a_{3,8} = -5.8235016129647971089$ | $a_{4,16} = -0.12549015561536110372$ |
| $a_{2,2} = 0.47007080279424540800$ | $a_{3,9} = -1.0472767830023645070$ | $a_{4,17} = -0.11250298507032009025$ |
| $a_{2,3} = 0.093589176759289320118$ | $a_{3,10} = 3.2615209891555982371$ | $a_{4,18} = 0.022964117700293735857$ |
| $a_{2,4} = 0.33386224041716468423$ | $a_{3,11} = 3.5478595826728208891$ | $a_{4,19} = 0.031709446610808019222$ |
| $a_{2,5} = -0.11418395501435496457$ | $a_{3,12} = 3.0921640208240511054$ | $a_{4,20} = -0.0032149051440245356510$ |
| $a_{2,6} = -0.18998278818813064037$ | $a_{3,13} = -0.34364793368678654581$ | $a_{4,21} = -0.0054335286230388551025$ |
| $a_{2,7} = 0.38484431284491986603$ | $a_{3,14} = -4.5566547247355317663$ | $a_{4,22} = 0.00022177994574852164638$ |
| | $a_{3,15} = -2.4329078834671892590$ | $a_{4,23} = 0.00042797426992744435493$ |

The interior of I_{F2C} is given by:

$$\begin{aligned}
 a_8 &= -0.0023556211403911721282 & a_3 &= -0.059814453125 \\
 a_7 &= -0.001220703125 & a_2 &= 0.13191478386190563918 \\
 a_6 &= 0.018844969123129377026 & a_1 &= 0.299072265625 \\
 a_5 &= 0.011962890625 & a_0 &= 0.33510652017261795103 \\
 a_4 &= -0.065957391930952819589
 \end{aligned}$$

III.8 Eighth- to Fourth-Order Case

The upper left corner of I_{F2C} is given by:

| | | |
|--|--|--|
| $a_{1,1} = 0.58483823651420605520$ | $a_{2,8} = 0.25040596791141593267$ | $a_{3,16} = -0.41961367860804052329$ |
| $a_{1,2} = 0.65474734710702549940$ | $a_{2,9} = 0.039631571628602904441$ | $a_{3,17} = 2.6138186452177357535$ |
| $a_{1,3} = -0.083569673821672843574$ | $a_{2,10} = -0.25355792154009083332$ | $a_{3,18} = 0.79040581189389266572$ |
| $a_{1,4} = 0.022425968859768418924$ | $a_{2,11} = -0.50801440584689113247$ | $a_{3,19} = -1.0153714219277431776$ |
| $a_{1,5} = 0.31477269554917488790$ | $a_{2,12} = -0.21961026714024651967$ | $a_{3,20} = -0.25660116699213786317$ |
| $a_{1,6} = -0.19106598818802213021$ | $a_{2,13} = 0.095341708111114624790$ | $a_{3,21} = 0.24235775601107244412$ |
| $a_{1,7} = -0.69007595018747002513$ | $a_{2,14} = 0.24893964119173768791$ | $a_{3,22} = 0.032202698057872206652$ |
| $a_{1,8} = -0.30500476635452414633$ | $a_{2,15} = 0.39235409374512417332$ | $a_{3,23} = -0.026566452015385539718$ |
| $a_{1,9} = 0.011380303429615219398$ | $a_{2,16} = 0.042074861655253219822$ | $a_{4,1} = 0.0085760788432811750313$ |
| $a_{1,10} = 0.39023505096198663290$ | $a_{2,17} = -0.34486664831340391286$ | $a_{4,2} = 0.013512845571180982502$ |
| $a_{1,11} = 0.69293443221288252711$ | $a_{2,18} = -0.10508512775619684648$ | $a_{4,3} = 0.022567253340913112846$ |
| $a_{1,12} = 0.27930147563078413713$ | $a_{2,19} = 0.13702066788245211707$ | $a_{4,4} = -0.058307759363885212745$ |
| $a_{1,13} = -0.17509858064671991258$ | $a_{2,20} = 0.035285372237949024781$ | $a_{4,5} = -0.12041195448680664419$ |
| $a_{1,14} = -0.36446581507281642455$ | $a_{2,21} = -0.033422056958152836350$ | $a_{4,6} = 0.22948717483369626712$ |
| $a_{1,15} = -0.53431810490188879575$ | $a_{2,22} = -0.0045282849361975826191$ | $a_{4,7} = 0.54863763561981341312$ |
| $a_{1,16} = -0.047645255801647499040$ | $a_{2,23} = 0.0037357262504306790489$ | $a_{4,8} = 0.41924435198770363142$ |
| $a_{1,17} = 0.48950384943343111452$ | $a_{3,1} = -0.095787414722590617699$ | $a_{4,9} = 0.25222427818457038144$ |
| $a_{1,18} = 0.14968600350317559693$ | $a_{3,2} = -0.68323289165328697626$ | $a_{4,10} = -0.029868530356228792693$ |
| $a_{1,19} = -0.19713593239026365497$ | $a_{3,3} = -0.43569930844225202810$ | $a_{4,11} = -0.30540634608037589943$ |
| $a_{1,20} = -0.051374514632076414476$ | $a_{3,4} = 1.8027331550089460412$ | $a_{4,12} = -0.18020289186124353787$ |
| $a_{1,21} = 0.048757624195804968082$ | $a_{3,5} = 3.7567210660509388125$ | $a_{4,13} = -0.015353428793734303657$ |
| $a_{1,22} = 0.0066939070511429668639$ | $a_{3,6} = -0.040511780395060609101$ | $a_{4,14} = 0.10180220964078586702$ |
| $a_{1,23} = -0.0055223124518961777586$ | $a_{3,7} = -3.9354784185565657354$ | $a_{4,15} = 0.23447509646113431046$ |
| $a_{2,1} = 0.011443922859934377398$ | $a_{3,8} = -2.5330463966461275528$ | $a_{4,16} = 0.040929410205375688302$ |
| $a_{2,2} = 0.37277008707234857179$ | $a_{3,9} = -1.0862631313184671074$ | $a_{4,17} = -0.17564595949066362349$ |
| $a_{2,3} = 0.35282527696092662640$ | $a_{3,10} = 1.5476108406776833914$ | $a_{4,18} = -0.051894216445801530355$ |
| $a_{2,4} = 0.096066986437174930272$ | $a_{3,11} = 4.0781324522987606857$ | $a_{4,19} = 0.065022578066260344054$ |
| $a_{2,5} = -0.22996810860646674853$ | $a_{3,12} = 1.9733308525923243475$ | $a_{4,20} = 0.015872184741392310993$ |
| $a_{2,6} = 0.12123432064337482341$ | $a_{3,13} = -0.37565017560062195914$ | $a_{4,21} = -0.014923762934166461295$ |
| $a_{2,7} = 0.49992261650980671917$ | $a_{3,14} = -1.7659882182232900992$ | $a_{4,22} = -0.0019211515134671124718$ |
| | $a_{3,15} = -3.1675028227076565595$ | $a_{4,23} = 0.0015849038302656338915$ |

The interior of I_{F2C} is given by:

$$\begin{aligned}
 a_8 &= -0.0087234986549392520415 & a_3 &= 0.018424137003272281874 \\
 a_7 &= 0.010574245783011317441 & a_2 &= 0.12963112574463663703 \\
 a_6 &= 0.041177278191813548941 & a_1 &= 0.25870815444749646286 \\
 a_5 &= -0.037706537233780062173 & a_0 &= 0.35615551493294340455 \\
 a_4 &= -0.090162662747982636209
 \end{aligned}$$

References

- [1] S. Abarbanel and A. Ditkowski. Asymptotically stable fourth-order accurate schemes for the diffusion equation on complex shapes. *J. Comput. Phys.*, 133:279–288, 1997.
- [2] A. Bayliss, K. E. Jordan, B. J. Lemesurier, and E. Turkel. A fourth order accurate finite difference scheme for the computation of elastic waves. *Bull. Seismol. Soc. Amer.*, 76(4):1115–1132, 1986.
- [3] M. H. Carpenter, D. Gottlieb, and S. Abarbanel. Time-stable boundary conditions for finite-difference schemes solving hyperbolic systems: Methodology and application to high-order compact schemes. *J. Comput. Phys.*, 111(2), 1994.
- [4] M. H. Carpenter, J. Nordström, and D. Gottlieb. A Stable and Conservative Interface Treatment of Arbitrary Spatial Accuracy. *J. Comput. Phys.*, 148, 1999.
- [5] Peter Diener, Ernst Nils Dorband, Erik Schnetter, and Manuel Tiglio. Optimized high-order derivative and dissipation operators satisfying summation by parts, and applications in three-dimensional multi-block evolutions. *J. Sci. Comput.*, 32(1):109–145, 2007.
- [6] B. Gustafsson. The convergence rate for difference approximations to general mixed initial boundary value problems. *SIAM J. Numer. Anal.*, 18(2):179–190, Apr. 1981.
- [7] B. Gustafsson, H.-O. Kreiss, and J. Oliger. *Time dependent problems and difference methods*. John Wiley & Sons, Inc., 1995.
- [8] B. Gustafsson, H. O. Kreiss, and A. Sundström. Stability theory of difference approximations for mixed initial boundary value problems. *Math. Comp.*, 26(119), 1972.

- [9] B. Gustafsson and P. Olsson. Fourth-order difference methods for hyperbolic IBVPs. *J. Comput. Physics*, 117(1), 1995.
- [10] J.S. Hesthaven. A stable penalty method for the compressible Navier-Stokes equations: II Multi-dimensional domain decomposition schemes. *SIAM J.Sci.Comput.*, 1998.
- [11] D. A. Kopriva and J. H. Kolas. A conservative staggered-grid chebyshev multidomain method for compressible flows. *J. Comput. Phys.*, 125(1):244–261, 1996.
- [12] H.-O. Kreiss and G. Scherer. Finite element and finite difference methods for hyperbolic partial differential equations. *Mathematical Aspects of Finite Elements in Partial Differential Equations.*, Academic Press, Inc., 1974.
- [13] Heinz-Otto Kreiss and Joseph Oliger. Comparison of accurate methods for the integration of hyperbolic equations. *Tellus XXIV*, 3, 1972.
- [14] L. Lehner, O. Reula, and M. Tiglio. Multi-block simulations in general relativity: high-order discretizations, numerical stability and applications. *Classical Quantum Gravity*, 22:5283–5321, 2005.
- [15] S. K. Lele. Compact finite difference schemes with spectral-like resolution. *J. Comput. Phys.*, 103:16–42, 1992.
- [16] K. Mattsson. Boundary procedures for summation-by-parts operators. *Journal of Scientific Computing*, 18:133–153, 2003.
- [17] K. Mattsson, F. Ham, and G. Iaccarino. Stable and accurate wave propagation in discontinuous media. *J. Comput. Phys.*, In Press, 2008.
- [18] K. Mattsson and J. Nordström. Summation by parts operators for finite difference approximations of second derivatives. *J. Comput. Phys.*, 199(2):503–540, 2004.
- [19] K. Mattsson and J. Nordström. High order finite difference methods for wave propagation in discontinuous media. *J. Comput. Phys.*, 220:249–269, 2006.
- [20] K. Mattsson, M. Svärd, M.H. Carpenter, and J. Nordström. High-order accurate computations for unsteady aerodynamics. *Computers & Fluids*, 36:636–649, 2006.

- [21] K. Mattsson, M. Svärd, and J. Nordström. Stable and Accurate Artificial Dissipation. *Journal of Scientific Computing*, 21(1):57–79, August 2004.
- [22] K. Mattsson, M. Svärd, and M. Shoeybi. Stable and accurate schemes for the compressible navier-stokes equations. *J. Comput. Phys.*, 227(4):2293–2316, 2008.
- [23] J. Nordström and M. H. Carpenter. Boundary and interface conditions for high-order finite-difference methods applied to the Euler and Navier-Stokes equations. *J. Comput. Phys.*, 148:341–365, 1999.
- [24] J. Nordström and M. H. Carpenter. High-order finite difference methods, multidimensional linear problems, and curvilinear coordinates. *J. Comput. Phys.*, 173:149–174, 2001.
- [25] J. Nordström and J. Gong. A stable hybrid method for hyperbolic problems. *J. Comput. Phys.*, 212:436–453, 2006.
- [26] J. Nordström, K. Mattsson, and R.C. Swanson. Boundary conditions for a divergence free velocity-pressure formulation of the incompressible navier-stokes equations. *J. Comput. Phys.*, 225:874–890, 2007.
- [27] P. Olsson. Summation by parts, projections, and stability I. *Math. Comp.*, 64:1035, 1995.
- [28] P. Olsson. Summation by parts, projections, and stability II. *Math. Comp.*, 64:1473, 1995.
- [29] S. De Rango and D. W. Zingg. High-order aerodynamic computations on multi block grids. *AIAA Paper*, 2001-2631, 2001.
- [30] B. Sjogreen. High order centered difference methods for the compressible navier-stokes equations. Technical report 01.01, RIACS, NASA Ames Research Center, 2001.
- [31] B. Strand. Summation by parts for finite difference approximations for d/dx . *J. Comput. Physics*, 110:47–67, 1994.
- [32] John C. Strikwerda. High-order-accurate schemes for incompressible viscous flow. *International Journal for Numerical Methods in Fluids*, 24:715–734, 1997.

- [33] M. Svärd, M. H. Carpenter, and J. Nordström. A stable high-order finite difference scheme for the compressible Navier–Stokes equations, far-field boundary conditions. *J. Comput. Physics*, 225:1020–1038, February 2008.
- [34] M. Svärd, M. H. Carpenter, and J. Nordström. A stable high-order finite difference scheme for the compressible Navier–Stokes equations, no-slip wall boundary conditions. *J. Comput. Physics*, 227:4805–4824, May 2008.
- [35] M. Svärd, K. Mattsson, and J. Nordström. Steady-state computations using summation-by-parts operators. *Journal of Scientific Computing*, 24(1):79–95, July 2005.
- [36] M. Svärd and J. Nordström. On the order of accuracy for difference approximations of initial-boundary value problems. *J. Comput. Physics*, 218:333–352, October 2006.
- [37] D. W. Zingg, S. De Rango, M. Nemec, and T. H. Pulliam. Comparison of several spatial discretizations for the Navier-Stokes equations. *AIAA Paper*, 99-3260, 1999.